Macromolecules

Article

pubs.acs.org/Macromolecules

Preparation of a High-Strength Hydrogel with Slidable and Tunable Potential Functionalization Sites

Zhao Li, Zhen Zheng, Shan Su, Lin Yu, and Xinling Wang*

School of Chemistry and Chemical Engineering, State Key Laboratory of Metal Matrix Composites, Shanghai Jiao Tong University, 800 Dongchuan Road, Shanghai 200240, China

Supporting Information

ABSTRACT: A hydrogel with tunable potential functionalization sites has been successfully prepared. As potential functionalization sites, (2-hydroxypropyl)-α-CDs (Hy-α-CDs) were introduced into the network of tetrahedron-like poly(ethylene glycol) (tetra-PEG) gel through supramolecular chemistry. In the stage of complexation, poly-*pseudo*-rotaxane consisting of tetra-PEG macromonomer and Hy-α-CD formed in pregel solution. The dynamic complexation process and the structure of the poly-*pseudo*-rotaxane were investigated by NMR experiment. In the stage of gelation, some cross-linking reactions were completed through click chemistry. The structures and mechanical properties of the resultant hydrogels were characterized by ATR-FTIR, XPS, SEM, and compression test in detail. The number of Hy-α-CD introduced into the hydrogel is related closely to the structure of the poly-*pseudo*-rotaxane and can be controlled easily by tuning the feed ratio. Anthracene as an example of function was introduced into the hydrogel through Hy-α-CD to preliminarily demonstrate the validity of the potential functionalization site in the last, and the hydrogel also has the capacity for further diverse functionalization.

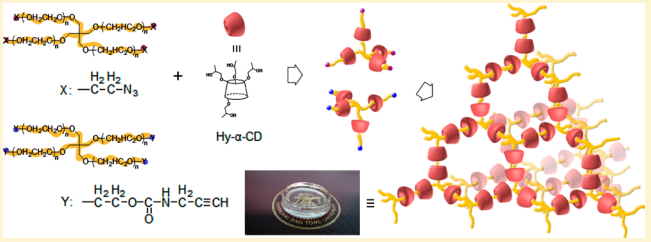

INTRODUCTION

Hydrogels are three-dimensional polymer networks containing a large amount of water inside.[1] They play important roles in many areas, such as medical treatment,[2,3] actuators,[4] cosmetics,[5] sewage disposal,[6] and so on. To be applied in a more complicated and sophisticated way, hydrogel ought to be stronger and more functional. On the other hand, the network structure of hydrogel should be regular and clear so that the properties of it can be controlled easily.

Over the past decade, hydrogels with high mechanical strength came through fast development.[7] Nanocomposite gel,[8] macromolecular microsphere composite gel,[9] double network gel,[10] slide-ring gel,[11−13] and tetrahedron-like poly(ethylene glycol) gel (tetra-PEG gel)[14] all own excellent mechanical properties. Among them, tetra-PEG gel has high strength due to its ideally homogeneous network structure.[15−20] To expand the application fields of the tetra-PEG gel, it is necessary to functionalize it. However, chemical inertness of PEG backbone limits its modification, which could only be realized through linking functional groups to termini of tetra-PEG macromonomer.[21] With this method, not only is the number of functional group limited, but the mechanical properties of the hydrogel are impacted.[21] Hence, introducing enough functionalization sites through an effective way is critical to functionalize tetra-PEG gel.

Cyclodextrins (CDs) are toroid-shaped cyclic oligomers of anhydroglucopyranose[22] full of hydroxyl groups, with the primary hydroxyl groups at the narrow side and the secondary hydroxyl groups at the wide side. Those CDs consisting of six, seven, or eight glucose units are α-, β-, or γ-CDs. One of the significant features of these CDs is that they are able to be chemically modified by a wide variety of methods,[23,24] which figures CD to be one of the essential roles in chemistry and material science. On the other hand, CDs can form inclusion complexes with many kinds of polymers.[25] In 1990, it was found that PEG and α-CD could form crystalline poly-*pseudo*-rotaxane and separated out from water.[26] The size matching of the cross-sectional area of PEG chain and the interior cavity of α-CD make formation of the poly-*pseudo*-rotaxane possible, and the major driving forces of the complexation are hydrophobic and van der Waals interactions between the inner surface of the α-CD ring and the hydrophobic sites on PEG.[25]

α-CD seems to be the appropriate candidate for the potential functionalization site. This is similar to slide-ring gel, the network chains in which are interlocked by figure-of-eight cross-links.[27] The figure-of-eight structure is made up of two linked α-CDs.[28] However, the solubility of α-CD/PEG poly-*pseudo*-rotaxane is limited by the formation of hydrogen bonding through hydroxyl groups between adjacent α-CDs. The homogeneous network structure of tetra-PEG gel would be undoubtedly affected if crystalline poly-*pseudo*-rotaxane exists. (2-Hydroxypropyl)-α-CD is a common α-CD derivative broadly used in drug formulation due to its high water solubility and excellent biocompatibility,[29] and we found that it could

Received: October 30, 2015
Revised: December 19, 2015

DOI: 10.1021/acs.macromol.5b02359
Macromolecules XXXX, XXX, XXX−XXX

form poly-*pseudo*-rotaxane with PEG with any molar ratio without crystalline during research. Therefore, we chose it as the potential functionalization site.

Herein, a novel hydrogel with high **strength**, ideally homogeneous network **structure**, and **slidable** potential functionalization site, (2-hydroxypropyl)-*α*-CD (**Hy-*α*-CD**), was developed. We abbreviated it to *α*SSS hydrogel based on the bold words above. The hydrogel's skeleton is based on tetra-PEG gel. Hy-*α*-CD was introduced into the hydrogel through supramolecular chemistry. Two stages including complexation and gelation were involved in the preparation of the hydrogel. In the stage of complexation, Hy-*α*-CD and tetra-PEG macromonomers formed poly-*pseudo*-rotaxane in a pregel solution. In the stage of gelation, the equilibrated pregel solution was cross-linked *in situ* by copper(I)-catalyzed azide−alkyne cycloaddition (CuAAC) click chemistry.[30,31] The number of Hy-*α*-CD introduced into the *α*SSS hydrogel is related to the structure of the poly-*pseudo*-rotaxane and can be controlled easily by tuning the feed ratio. In addition, the existence of Hy-*α*-CD changes the morphology and increases the mechanical properties of the hydrogel. Since the constitutional tetra-PEG macromonomers and Hy-*α*-CD are biocompatible, the *α*SSS hydrogel has prospect to be used as a biomaterial. In the last, anthracene as an example of function unit was introduced into the *α*SSS hydrogel to briefly demonstrate the validity of the potential functionalization sites of Hy-*α*-CD in the hydrogel. The obtained functionalized *α*SSS hydrogel (An-*α*SSS hydrogel) possesses fluorescence.

EXPERIMENTAL SECTION

Materials. Tetrahydroxyl-terminated PEG (THPEG) (M_w = 20 000) was obtained from Sinopeg Biotech Co., Ltd., and dried in a vacuum with magnetic stirring at 85 °C for 2 h before use. (2-Hydroxypropyl)-*α*-CD (Hy-*α*-CD) (M_w ∼ 1180) with substitution degree about 3.6 was obtained from Sigma-Aldrich Corp. and dried in a vacuum at 85 °C before use. Propargylamine, 4-(dimethylamino)-pyridine (DMAP), *p*-toluenesulfonyl chloride (TsCl), sodium azide (NaN_3), triphosgene (BTC), deuterium oxide (D_2O), tetramethylammonium (TMA) chloride, copper sulfate pentahydrate ($CuSO_4·5H_2O$), and sodium ascorbic acid of analytical grade were obtained from Sigma-Aldrich Corp. and used as-received. 2-Amineanthracene was synthesized through the reduction of 2-aminoanthraquinone (Aladdin Industrial Co., Ltd.) according to the method in ref 32. Dichloromethane (DCM) and chloroform were obtained from Sigma-Aldrich Corp. and dried with 4A molecular sieve. Dimethylformamide (DMF) and trimethylamine (TEA) were obtained from Sigma-Aldrich Corp. and distilled with CaH_2 before use.

Preparation of Terminal Modified Tetra-PEG Macromonomers. Tetra-toluenesulfonate-terminated PEG and tetra-azido-terminated PEG were prepared according to the method in refs 33 and 34. Tetra-propargyl-terminated PEG was prepared through the efficient reaction between −NCO on propargyl isocyanate and −OH on THPEG (Scheme S1). The structures of the products were determined by ^{1}H NMR (400 MHz) spectroscopy recorded on a Varian MERCURY plus-400 spectrometer at 25.0 ± 0.5 °C.

Preparation of Tetratoluenesulfonate-Terminated PEG (TTPEG). THPEG (5.0 g, 0.25 mmol), DMAP (3.66 g, 30 mmol), and TEA (7.5 mL) were dissolved in DCM (50 mL), and the solution was cooled to 0 °C under argon via an additional funnel. To this solution, TsCl (5.72 g, 30 mmol) dissolved in DCM (50 mL) was added dropwise in 15 min. The reaction was allowed to warm to room temperature overnight with magnetic stirring under argon. The solution was concentrated and washed with 0.5 M HCl aqueous solution. The organic layer was dried with magnesium sulfate and filtered. An excess amount of diethyl ether was added in filtrate to precipitate. After filtration, the product was precipitated twice in diethyl ether, filtered, and dried in a vacuum overnight. ^{1}H NMR (DMSO-d_6 with 0.03% v/v TMS, 400 MHz): δ 7.795 (d, 8H, 2-H of phenyl), 7.494 (d, 8H, 3-H of phenyl), 4.109 (t, 8H, Ts−O−CH_2−), 3.508 (m, 1794H, $[CH_2CH_2O]_n$), 2.424 (s, 12H, CH_3−phenyl−).

Preparation of Tetraazido-Terminated PEG (TAPEG). TTPEG (4.0 g, 0.19 mmol) and sodium azide (0.50 g, 7.76 mmol) were mixed in DMF (100 mL), and the solution was stirred under argon at 80 °C for 24 h. The solid salts were removed via filtration through Celite. The polymer was recovered via precipitation with diethyl ether and filtration thrice. The product was dried in vacuum overnight. ^{1}H NMR (DMSO-d_6 with 0.03% v/v TMS, 400 MHz): δ 3.506 (m, 1794H, $[CH_2CH_2O]_n$), 3.372 (t, 8H, N_3−CH_2−).

Preparation of Tetrapropargyl-Terminated PEG (TPPEG). BTC (2.04 g, 6.87 mmol) was dissolved in chloroform (40 mL), and the solution was cooled to −10 °C under argon via an additional funnel. To this solution, propargylamine (1.10 g, 20 mmol) and TEA (4.07 g, 40.3 mmol) that were all dissolved in chloroform (40 mL) were added dropwise in 45 min. The mixture was stirred at −10 °C for another 45 min under argon. Then the temperature was increased to 30 °C, and the mixture was stirred for 1 h. The solution was concentrated and washed with 0.5 M HCl aqueous solution. The organic layer was dried with magnesium sulfate and filtered. The filtrate was pour into THPEG's chloroform solution [THPEG (5.0 g, 0.25 mmol) and chloroform (100 mL)]. After stannous octanoate (0.005 g) was added, the solution was stirred at 60 °C under argon for 5 h. The solution was concentrated, and an excess amount of diethyl ether was added. The precipitate was precipitated twice in diethyl ether, filtered, and dried in a vacuum overnight. ^{1}H NMR (DMSO-d_6 with 0.03% v/v TMS, 400 MHz): δ 7.650 (t, 4H, −O−CO−NH−), 4.071 (t, 8H, −NHCOO−CH_2−), 3.682 (t, 8H, −NHCOO−CH_2−CH_2−), 3.508 (m, 1794H, $[CH_2CH_2O]_n$), 3.077 (s, 4H, CH≡C−).

Preparation of 2-Anthracenecarbamyl-Hy-*α*-CD (An-Hy-*α*-CD). First, 2-anthraceneisocyanate (2-An-NCO) was synthesized through isocyanation of 2-amineanthracene by the BTC method. BTC (1.25 g, 2.12 mmol) was dissolved in DCM, and the solution was cooled to −10 °C under argon. 2-Amineanthracene (1.22 g, 6.34 mmol) and TEA (1.25 g, 12.37 mmol) dissolved in DCM were added dropwise to this solution. The reaction was stirred at −10 and 30 °C for 1 h. The solution was washed with HCl aqueous solution, and the organic layer was dried with magnesium sulfate. Evaporation of all the DCM gave dark green solid of raw product of 2-An-NCO which was used directly in reaction with Hy-*α*-CD.

Then 2-anthracenecarbamyl-Hy-*α*-CD (Scheme 3) was synthesized through the reaction between 2-An-NCO and Hy-*α*-CD. The 2-An-NCO obtained above and Hy-*α*-CD (2.49 g, 2.11 mmol) were mixed in DMF. After stannous octanoate (0.01 g) was added, the solution was stirred at 60 °C under argon for 24 h. The solution was concentrated and precipitated in an excess amount of diethyl ether thrice. After the filtration, the precipitate washed with diethyl ether until the supernatant was colorless. Drying in vacuum overnight gives the product of 2-anthracenecarbamyl-Hy-*α*-CD. ^{1}H NMR (DMSO-d_6 with 0.03% v/v TMS, 400 MHz): δ 9.78 (−N*H*−COO−), 7.10−8.60 (anthracene), 5.30−6.20 O(2,2′,2″,3,3′,3″)H of Hy-*α*-CD, 5.00 O(8)H of Hy-*α*-CD, 4.60−5.20 C(1,1′,1″)H of Hy-*α*-CD, 4.53 O(6)H of Hy-*α*-CD, 3.10−4.20 C(2,2′,2″,3,3′,3″,4,4′,4″,5,5′,5″,6,6′,6″,7,8)H of Hy-*α*-CD, 1.03 C(9)H of Hy-*α*-CD.

Complexation between Hy-*α*-CD and Tetra-PEG Macromonomers in Pregel Solution. Nuclear magnetic resonance spectroscopy was used to characterize the complexation between Hy-*α*-CD and tetra-PEG macromonomers in a pregel solution. ^{1}H NMR (400 MHz) and ^{13}C NMR (100 MHz) spectra were recorded on a Varian MERCURY plus-400 spectrometer at 25.0 ± 0.5 °C with 64 and 1024 scans, respectively, for every sample. 2D NOESY NMR (400 MHz) spectra were obtained using a Bruker AVANCEIII 400 spectrometer with a mixing time of 300 ms at 25.0 ± 0.5 °C. The 2048 experiments were performed with four scans per experiment. THPEG was used as model macromonomer. Deuterium oxide was used as solvent with chloroform sealed in glass capillary of 1.0 mm diameter as an external reference. Samples for NMR experiment were listed in Table 1. **1a** to **6a** were used to simulate pregel solutions of the *α*SSS

DOI: 10.1021/acs.macromol.5b02359
Macromolecules XXXX, XXX, XXX−XXX

Table 1. Compositions of Samples for NMR Experiment

sample	solute	solvent	$n_{\text{Hy-}\alpha\text{-CD}}:n_{\text{THPEG}}$	$m_{D_2O}:m_{\text{THPEG}}$	$c_{\text{Hy-}\alpha\text{-CD}}$[a] (mmol/g)
0a	THPEG	D_2O		9	
1a	THPEG, Hy-α-CD	D_2O	5	9	0.02689
2a	THPEG, Hy-α-CD	D_2O	10	9	0.05213
3a	THPEG, Hy-α-CD	D_2O	25	9	0.1193
4a	THPEG, Hy-α-CD	D_2O	50	9	0.2097
5a	THPEG, Hy-α-CD	D_2O	75	9	0.2799
6a	THPEG, Hy-α-CD	D_2O	100	9	0.3362
1a(Blank)	Hy-α-CD	D_2O			0.02689
2a(Blank)	Hy-α-CD	D_2O			0.05213
3a(Blank)	Hy-α-CD	D_2O			0.1193
4a(Blank)	Hy-α-CD	D_2O			0.2097
5a(Blank)	Hy-α-CD	D_2O			0.2799
6a(Blank)	Hy-α-CD	D_2O			0.3362

[a] $c_{\text{Hy-}\alpha\text{-CD}} = n_{\text{Hy-}\alpha\text{-CD}}/(m_{\text{Hy-}\alpha\text{-CD}} + m_{D_2O})$.

Table 2. Some Parameters of Hydrogel Samples 0ag to 6ag

sample	$n_{\text{TAPEG}}:n_{\text{TPPEG}}$	M[a]	N_{initial}	$N_{\text{Hy-}\alpha\text{-CD}}$	SR (%)	EWC (%)
0ag	1	9	0	0 ± 0		95.4 ± 0.6
1ag	1	9	5	5.0 ± 0.6	100 ± 12.0	94.6 ± 0.5
2ag	1	9	10	9.9 ± 0.5	99 ± 5.0	95.3 ± 1.1
3ag	1	9	25	22.0 ± 1.0	88.4 ± 4.0	95.3 ± 1.0
4ag	1	9	50	30.0 ± 2.1	60.4 ± 4.2	94.7 ± 1.0
5ag	1	9	75	36.9 ± 3.2	49.6 ± 4.3	94.8 ± 1.2
6ag	1	9	100	48.3 ± 5.0	48.7 ± 5.0	94.8 ± 0.7

[a] M represents the mass ratio of DI water to tetra-PEG macromonomers (TAPEG and TPPEG) ($m_{\text{DI water}}:m_{\text{macromonomer}}$).

hydrogels and had same composition and equal feed ratios corresponding to the hydrogel samples **1ag** to **6ag** in Table 2. The mass ratio of D_2O to THPEG ($m_{D_2O}:m_{\text{THPEG}}$) was kept at 9, whereas the molar ratio of Hy-α-CD to THPEG ($n_{\text{Hy-}\alpha\text{-CD}}:n_{\text{THPEG}}$) changed from 5 to 100. Sample **0a** was THPEG's D_2O solution without Hy-α-CD, and it was the reference to calculate the chemical shift variation ($\Delta\delta$) of THPEG. Hy-α-CD could form intermolecular inclusion complexes in aqueous solution and its complexation behavior had concentration dependency. Thus, blank samples **1a(Blank)** to **6a(Blank)** of Hy-α-CD's D_2O solution without THPEG were prepared, the concentrations of which were equal to samples **1a** to **6a**, respectively. They were used as references to elucidate the changes of Hy-α-CD's structure before and after the addition of THPEG under different Hy-α-CD concentrations.

The chemical shifts of all protons of CDs decrease linearly with the increase of CD concentration.[35] In addition, with the existence of CDs, internal reference compounds were reported to show significant downfield shifts during NMR titration experiments.[36] During this research, it was found not only small molecules but polymers like THPEG of which all protons decreased linearly with the increase of Hy-α-CD's concentration. Furthermore, ^{13}C of Hy-α-CD, THPEG, and internal references also showed downfield shifts during NMR experiments. These phenomena may be the consequence of changes in the magnetic susceptibilities of water due to hydrogen bonding with the glucose units of the cyclodextrin.[37] Accordingly, chloroform was used as external reference to correct the data from ^1H and ^{13}C NMR spectra.

Monitoring the Complexation Process between Hy-α-CD and THPEG. ^1H NMR spectrometry was used to monitor the process of the complexation between Hy-α-CD and THPEG. During the experiment, certain amounts of Hy-α-CD and THPEG were dissolved in D_2O according to the compositions of **1a** to **6a**, and these six samples were incubated at 37 °C. ^1H NMR spectra were taken every a certain period of time until 254.0 h.

Characterization of the Poly-Pseudo-Rotaxane at Dynamic Equilibrium. ^1H, ^{13}C, and 2D NOESY NMR spectrometry were used to determine the structure of the poly-*pseudo*-rotaxane. Complexation between Hy-α-CD and THPEG needed time to reach the equilibrium after which the structure of the poly-*pseudo*-rotaxane was characterized.

Preparation of αSSS Hydrogel. A series of hydrogels **1ag** to **6ag** were prepared (Table 2). The molar ratio of TAPEG to TPPEG ($n_{\text{TAPEG}}:n_{\text{TPPEG}}$) of them was kept constant of 1:1, and the mass ratio of DI water to macromonomers (TAPEG and TPPEG) ($m_{\text{DI water}}:m_{\text{macromonomers}}$) was kept at 9:1. The molar ratios (feed ratios) of Hy-α-CD to macromonomers (N_{Initial}) changed from 5 to 100. Tetra-PEG hydrogel **0ag** without any Hy-α-CD was as blank sample to compare with αSSS hydrogel samples.

To a series of small vials were added TAPEG (0.1000 g, 4.975 μmol), TPPEG (0.1011 g, 4.975 μmol), and DI water (1.7599 g). After the macromonomers were dissolved, a different amount of Hy-α-CD was added to form pregel solution. The solutions were incubated at 37 °C. After the pregel solution reached the equilibrium, copper sulfate (1.592 mg, 9.950 μmol) in DI water (48.41 mg) and sodium ascorbate (9.8 mg, 49.5 μmol) were added. The vials were placed in an oven present to 37 °C. The hydrogels formed within minutes and stood for another 48 h, which were then treated with 0.5 M aqueous ethylenediaminetetraacetic acid (EDTA) solution followed by plenty of water to remove the copper catalysis and unthreaded Hy-α-CD. The hydrogels were incubated in DI water to fully swell before characterizations.

Characterizations of αSSS Hydrogel. *ATR-FTIR Measurement.* Attenuated total reflectance−Fourier transform infrared (ATR-FTIR) spectra were recorded on a Paragon 1000 instrument equipped with ATR accessory. The scan range was 4000 to 660 cm^{-1}, and seven scans were collected for each sample with a resolution of 2 cm^{-1}. The hydrogel samples were frozen in liquid nitrogen and broken. After freeze-drying, the sectioned surfaces were caught out ATR examination. Peak intensities of the αSSS hydrogels **1ag** to **6ag** were normalized to the C═O in carbamate group of pristine tetra-PEG hydrogel **0ag**.

XPS Measurement. Chemical composition of the sectioned surfaces of the hydrogel samples were analyzed using a Shimadzu-Kratos (AXIS

DOI: 10.1021/acs.macromol.5b02359
Macromolecules XXXX, XXX, XXX−XXX

Scheme 1. (a) Fabrication Process of the αSSS Hydrogel and (b) the Photograph of Hydrogel Sample 5ag

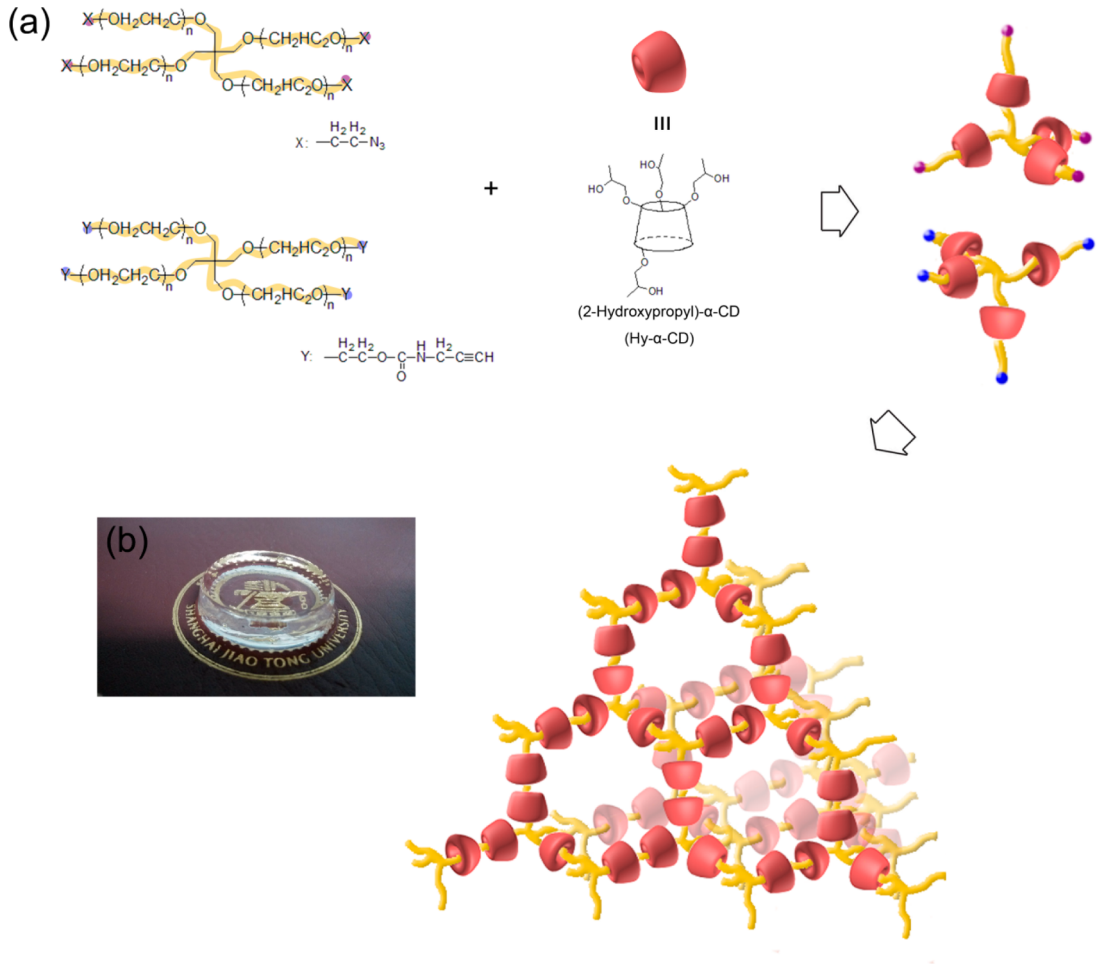

Ultra) X-ray photoelectron spectrometer (XPS) equipped with monochromatic Al Kα X-rays. A takeoff angle of 90° was employed for each sample. The scan area is 300 × 700 μm. At least three random positions on the sectioned surface of every hydrogel sample were chosen to be executed with XPS measurement. Initial representative survey scans were acquired from 0 to 1200 eV for three sweeps (sw). For further elemental analysis, high-resolution scans were acquired for the C 1s (~276 to 298 eV, 3 sw), O 1s (~524 to 543 eV, 2 sw), and N 1s (~392 to 412 eV, 12 sw) regions. For all spectra, the backgrounds of all regions were subtracted using the Shirley background.[38] Peak positions were normalized to the C 1s peak at 285.0 eV. The data analysis was carried out by using XPSPeak 4.1 software.

Swelling Measurement. The hydrogel samples were freeze-dried and then immersed in DI water for 3 days at room temperature to fully swell. The equilibrium water contents (EWCs) of the hydrogels were calculated by the following equation:

$$\mathrm{EWC} = \frac{m_{\mathrm{wet}} - m_{\mathrm{dry}}}{m_{\mathrm{wet}}} \times 100\% \quad (1)$$

At least three parallel samples were recorded for each hydrogel specimen.

Internal Morphology. The internal morphologies of the sectioned surfaces of the freeze-dried hydrogel samples were observed using a Philips Sirion 200 instrument scanning electron microscope (SEM). Photographs were taken with a Canon IXUS 800IS digital camera. The dried hydrogel samples were mounted on metal holder and vacuum coated with a gold layer prior to SEM examination.

Compression Test. A MTS Criterion 43 universal texting machine was used to measure mechanical performance of the αSSS hydrogel. Compression mode was used. A cylindrical sample about 7 mm in diameter and 5 mm in initial thickness was placed on a metal plate coated with silicon oil to decrease the friction.[39] The cross-head speeds was 1.0 mm/min. At least five parallel samples were recorded for each specimen the test.

Preparation of An-αSSS Hydrogel. TAPEG and TPPEG with equal moles were dissolved in DI water to get a 10 wt % solution. Then An-Hy-α-CD was added to the solution. After incubation at 37 °C for 120 h, copper sulfate and sodium ascorbate were added, and the solution was incubated at 37 °C for another 48 h to obtain a hydrogel. The hydrogel was treated with EDTA aqueous solution, DI water, and DMF to remove the copper catalysis and unthreaded An-Hy-α-CD. The gel was treated with DI water again to displace DMF and fully swollen in DI water before characterization.

Characterizations of An-αSSS Hydrogel. *UV−Vis DRS Measurement.* A PerkinElmer Lambda 750S UV/vis/NIR spectrophotometer equipped with a 60 mm integrating sphere was used to record the UV−vis diffuse reflectance spectrum of An-αSSS hydrogel. The scan range is 200−700 nm with step of 1 nm. The slit width is 2.0 nm. Polytetrafluoroethylene (PTFE) was used as a reflection standard. A cylinder-shaped hydrogel sample with diameter of 15 mm and height of 3 mm was sandwiched in two quartz plates, and the "sandwich" was placed in the sample compartment of the spectrometer.

Fluorescence Spectroscopy. Fluorescent excitation and emission spectra were recorded at room temperature using a PerkinElmer LS 55 fluorospectrometer with a solid sample holder with emission and excitation wavelength of 440 and 360 nm, respectively. The working voltage was 725 V, and the slit width was 7.5 nm. A cylinder-shaped hydrogel sample with diameter of 15 mm and height of 3 mm was sandwiched in two quartz plates, and the "sandwich" was placed in the sample holder.

DOI: 10.1021/acs.macromol.5b02359
Macromolecules XXXX, XXX, XXX−XXX

RESULTS AND DISCUSSION

Matrix of αSSS Hydrogel. The matrix of the αSSS hydrogel is tetra-PEG gel with regular and homogeneous network structure which is the origin of high strength and enables Hy-α-CDs to distribute evenly. To avert the influence of hydroxyl group on Hy-α-CD, classical "CuAAC" click chemistry was used as cross-linking reaction considering its unique characteristics of quantitative yields and high tolerance of functional groups. As for the synthesis of TAPEG, −OH groups at termini of THPEG were first activated by the tosyl group and then reacted with NaN_3. As for the synthesis of TPPEG, propargylamine was converted to propargyl isocyanate and then linked to termini of THPEG (Scheme S1). It takes the advantage of high efficiency of the reaction between −NCO and −OH and makes the preparation of TPPEG easy. In the meantime, C═O in the carbamate group was taken as effective internal reference in ATR-FTIR examination to normalize the spectra.

Preparation of αSSS Hydrogel. Two symmetrical tetrahedron-like PEG macromonomers, TAPEG and TPPEG, derived from THPEG were dissolved in DI water together with different amount of Hy-α-CD to form a series of pregel solutions. After these pregel solutions reached dynamic equilibrium (determination of the time to reach the equilibrium is discussed in the latter part of NMR analysis), gelation was carried out. The resultant αSSS hydrogel is a colorless hydrogel with excellent transparency (Scheme 1b). That partly indicates the homogeneous network of tetra-PEG gel is inherited by the αSSS hydrogel. That also indicates introduction of Hy-α-CD does not cause any crystalline in the hydrogel.

Quantification of the Amount of Hy-α-CD Introduced in αSSS Hydrogel. As the potential functionalization site, Hy-α-CD in the αSSS hydrogel will certainly act as a key role on the functionalization of the hydrogel. Thus, at this stage determining how many Hy-α-CDs are introduced in the αSSS hydrogel appears particularly important. Here ATR-FTIR and XPS spectroscopy were used to determine this parameter.

ATR-FTIR spectroscopy was used to semiquantitatively determine the amount of Hy-α-CD introduced into the αSSS hydrogel. Figure 1 shows the ATR-FTIR spectra of the sectioned surfaces of freeze-dried hydrogel samples **0ag** to **6ag**. In the figure, tetra-PEG hydrogel **0ag** provides a baseline. C−O−C stretching of poly(ethylene oxide) network appears peak at around 1100 cm^{-1}. A peak at 1721 cm^{-1} is for the C═O in carbamate group, which was used as the internal reference. Spectra in Figure 1 are normalized spectra. With the introduction of Hy-α-CD, the broad peak of hydroxyl group at around 3370 cm^{-1} appears. C−O−C stretching of Hy-α-CD arises at 1030 cm^{-1}. These results indicate that Hy-α-CDs are confined in hydrogel's network. It is also found that with increasing the amount of fed Hy-α-CD, peaks of hydroxyl and C−O−C group of Hy-α-CD strengthen gradually from **1ag** to **6ag**. This suggests that with the increase of fed Hy-α-CD in pregel solution, the amount of it confined in network of the hydrogel increases.

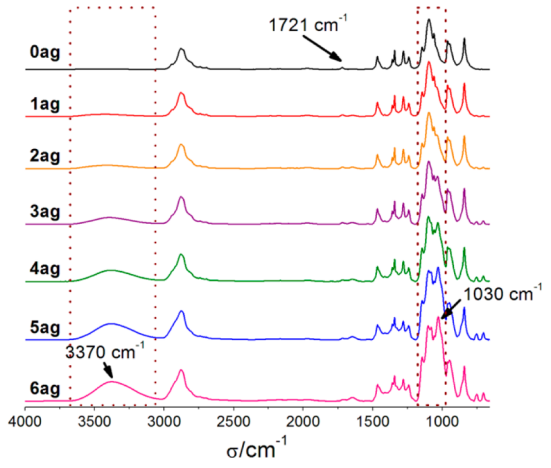

Figure 1. ATR-FTIR spectra of the sectioned surfaces of freeze-dried hydrogel samples **0ag** to **6ag**.

XPS was used to quantitatively determine the amount of Hy-α-CD introduced into the αSSS hydrogel. Typical high-resolution narrow scans of the C 1s regions of **0ag** to **6ag** are shown in Figure 2. After spectral fitting, in **0ag** spectrum, the peak at 285.0 eV is attributed to contaminate carbon and the peak at 286.6 eV is C(C−O/C−N) region of poly(ethylene oxide) network. In spectra of **1ag** to **6ag**, new peaks at 288.1 eV appear which are attributed to anomeric C(O−C−O) of Hy-α-CD, and the peaks at 286.5 eV correspond to C−O/C−N of poly(ethylene oxide) and Hy-α-CD. The peaks at 285.0 eV are attributed to C−C/C−H of Hy-α-CD and contaminate carbon.

The number of Hy-α-CD corresponding to every tetra-PEG macromonomer (TAPEG or TPPEG) ($N_{\text{Hy-}\alpha\text{-CD}}$) is used to express the amount of Hy-α-CD confined in the αSSS hydrogel's network. $N_{\text{Hy-}\alpha\text{-CD}}$ is defined as

$$N_{\text{Hy-}\alpha\text{-CD}} = \frac{n_{\text{Hy-}\alpha\text{-CD}}}{n_{\text{macromonomer}}} \tag{2}$$

Here $n_{\text{Hy-}\alpha\text{-CD}}$ and $n_{\text{macromonomer}}$ stand for moles of Hy-α-CD and tetra-PEG macromonomer in the hydrogel's network.

The αSSS hydrogel contains equal amount of TAPEG and TPPEG macromonomers. One TAPEG has 907 C−O/C−N type carbons. One TPPEG has 919 C−O/C−N type carbons. The average number of C−O/C−N type carbon contained in a tetra-PEG macromonomer is 913 (N_M).

One α-CD consists of $N_{CD} = 6$ glucopyranose units. In a Hy-α-CD molecule with 2-hydroxypropyl-substituted degree of 3.6, one glucopyranose unit contains 1 O−C−O type carbon, 6.2 C−O type carbons, and 0.6 C−C/C−H type carbons on average. In the XPS spectrum, peak area is in proportion to atom mole. Thus, in a αSSS hydrogel's XPS C 1s spectrum, the area corresponding to macromonomer's C−O/C−N type carbon is $(A_{286.6\text{ eV}} - A_{288.1\text{ eV}} \times 6.2)$, where $A_{286.6\text{ eV}}$ and $A_{288.1\text{ eV}}$ represent areas of peaks at 286.6 and 288.1 eV. $N_{\text{Hy-}\alpha\text{-CD}}$ can be written as

$$N_{\text{Hy-}\alpha\text{-CD}} = \frac{\frac{A_{288.1\text{ eV}}}{N_{CD}}}{\frac{A_{286.6\text{ eV}} - A_{288.1\text{ eV}} \times 6.2}{N_M}} \tag{3}$$

Putting $N_M = 913$ and $N_{CD} = 6$ into eq 3:

$$N_{\text{Hy-}\alpha\text{-CD}} = \frac{A_{288.1\text{ eV}} \times 152.2}{A_{286.6\text{ eV}} - A_{288.1\text{ eV}} \times 6.2} \tag{4}$$

According to eq 4, $N_{\text{Hy-}\alpha\text{-CD}}$ values of samples **1ag** to **6ag** were calculated and are listed in Table 2. The threading ratio (SR) of the αSSS hydrogel is defined as

$$\text{SR} = \frac{N_{\text{Hy-}\alpha\text{-CD}}}{N_{\text{initial}}} \times 100\% \tag{5}$$

DOI: 10.1021/acs.macromol.5b02359
Macromolecules XXXX, XXX, XXX−XXX

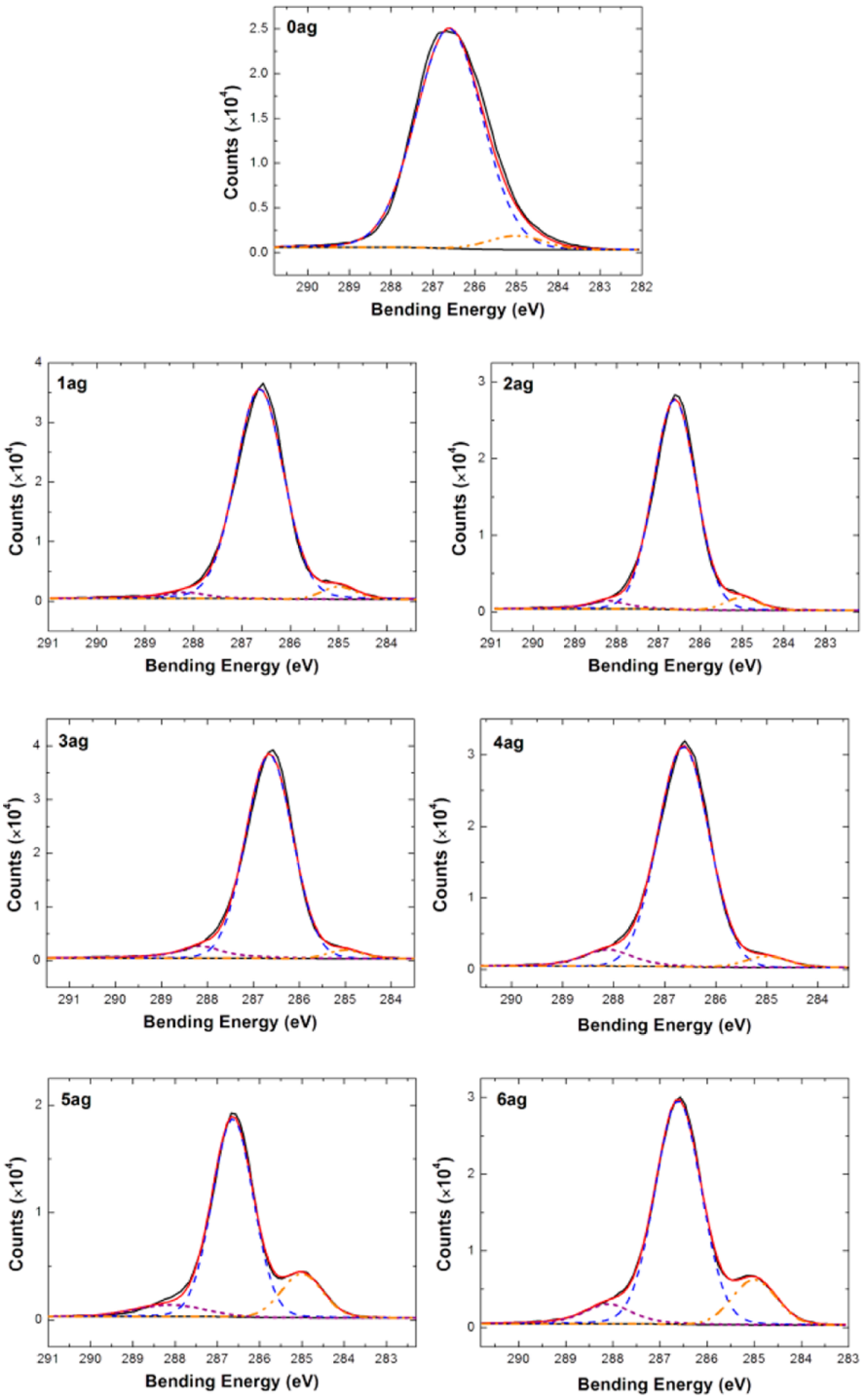

Figure 2. Typical XPS (C 1s) spectra for the sectioned surfaces of freeze-dried hydrogel samples **0ag** to **6ag**.

Here $N_{initial}$ is the number of Hy-α-CD corresponding to every macromonomer added initially in pregel solution.

From Table 2, it can be found that with the increase of the amount of fed Hy-α-CD in pregel solution, the number of Hy-α-CD confined in the αSSS hydrogel's network increases, and the threading efficiency of Hy-α-CD reduces.

Mechanism of Complexation between Hy-α-CD and Tetra-PEG Macromonomers in Pregel Solution. Complexation between Hy-α-CD and tetra-PEG macromonomers in pregel solution is the critical step for the preparation of the αSSS hydrogel. Clarifying the mechanism of the complexation is significant for preparation of the hydrogel with tunable amount of Hy-α-CD. On the basis of the obtained parameter of $N_{Hy\text{-}\alpha\text{-}CD}$ above, we are able to discuss the complexation mechanism combining it with the results of NMR experiment. TAGEG and TPPEG are derived from THPEG, and they have the same molecular weights as THPEG. So in the NMR experiment, THPEG was used as model macromonomer to complex with Hy-α-CD. NMR samples **1a** to **6a** have the same feed ratios of Hy-α-CD to tetra-PEG macromonomer and solute concentrations as the corresponding hydrogel samples **1ag** to **6ag** and were used to simulate the pregel solutions of

DOI: 10.1021/acs.macromol.5b02359
Macromolecules XXXX, XXX, XXX−XXX

1ag to **6ag**. The parameter of $N_{\text{Hy-}\alpha\text{-CD}}$ thus can be regarded as the amount of Hy-α-CD threaded on THPEG at dynamic equilibrium.

Although many reports on the preparation, characterization, and application of polymer/CD based poly-*pseudo*-rotaxanes and polyrotaxanes have been published, the threading mechanism and dynamics of a linear polymer in CDs have yet to be revealed.[40] However, this issue is essential and significant for dynamics of polymers in solution.[41,42] On the other hand, physical and chemical characters as well as behaviors in aqueous solution of Hy-α-CD are different from that of α-CD due to the substitution. And there are few researches about the complexation between polymers and substituted CD. Thus, clarification of complexation mechanism between Hy-α-CD and tetra-PEG is valuable to improve the theory of supramolecules.

Result of 2D NOESY ^{1}H NMR Measurement. 2D NOESY ^{1}H NMR spectroscopy is a straightforward method to determine the existence of host−guest interaction of organic compounds. It establishes correlation between nuclei of proton through nuclear Overhauser enhancement (NOE) effect. Hy-α-CD and THPEG were dissolved together in D_2O with different molar ratios (Table 1), and the solutions were incubated at 37 °C. After these NMR samples reached the dynamic equilibrium (a detailed description of the time to reach the dynamic equilibrium and the complexation process between Hy-α-CD and THPEG is being involved in the following part), 2D NOESY NMR spectra of them were taken.

Figure 3 shows a typical 2D NOESY ^{1}H NMR spectrum of the Hy-α-CD/THPEG system. In the 1D ^{1}H NMR spectrum in the figure, the signal around 3.73 ppm is assigned to the methylene proton of THPEG's monomeric CH_2CH_2O unit, and the signals around 4.00, 3.82, and 1.19 ppm are assigned to the protons of C(3)H, C(5)H, and C(9)H of Hy-α-CD, respectively (Scheme 2). As can be seen in the figure, signals of C(3)H and C(5)H of Hy-α-CD correlate with the resonance of the methylene proton of THPEG, which indicates that the host−guest interaction exists between Hy-α-CD and THPEG and the chains of THPEG are included in Hy-α-CDs' cavities. This complexation is driven by hydrophobic and van der Waals interactions between the inner surface of the Hy-α-CD ring and the hydrophobic sites on the chains of THPEG. Moreover, it is found that signal of C(9)H of Hy-α-CD correlates with the signal of methylene proton of THPEG. That indicates when Hy-α-CD threads on THPEG's chain, 2-hydroxypropyl groups of Hy-α-CD change their conformations to approach THPEG's chain and parallel with it at the equilibrium. In Figure 3b, it can be seen that signal of C(9)H also correlates with signals of C(3)H and C(5)H. When the feed ratio of Hy-α-CD to THPEG is greater than 10, the threading ratio (SR) of Hy-α-CD is less than 100% (Table 2). That means not all the fed Hy-α-CDs can thread on THPEG at the equilibrium, and there are unthreaded Hy-α-CDs in solution. These "free" Hy-α-CDs interact with each other to form intermolecular inclusion complexes in which 2-hydroxypropyl groups of one Hy-α-CD can insert into cavities of other Hy-α-CDs. Methyl parts on the 2-hydroxypropyl groups have hydrophobic interaction with C3 and C5 methines in the interior cavity of CD, which leads to the cross-peaks between C(9)H and C(3,5)H. This behavior of Hy-α-CD is also being demonstrated with the results of ^{13}C NMR experiment and discussed in the following part.

Complexation Process between Hy-α-CD and THPEG. In the ^{1}H NMR spectra of samples **1a** to **6a**, the methylene proton

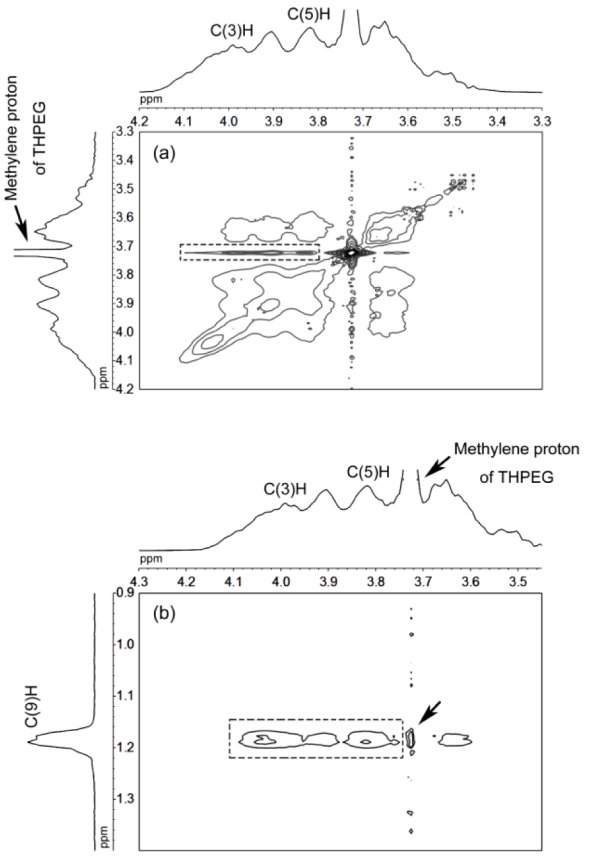

Figure 3. Partial 2D NOESY ^{1}H NMR spectra of sample **6a** at dynamic equilibrium.

of THPEG's monomeric CH_2CH_2O unit exhibits signal around 3.7 ppm (see Supporting Information). Figure 4 shows the chemical shift variations of the methylene protons ($\Delta\delta_{\text{THPEG}}$) as functions of time and molar ratio of Hy-α-CD to THPEG ($n_{\text{Hy-}\alpha\text{-CD}}$:$n_{\text{THPEG}}$). The positive variation indicates an increase in chemical shift δ, viz., a shift toward downfield, and vice versa. When THPEG was added to Hy-α-CD's aqueous solution, $\Delta\delta_{\text{THPEG}}$ values exhibited positive; that is, the ^{1}H resonance of the methylene proton shifted downfield. This indicates that Hy-α-CD threads on THPEG's chain and the exchange rate of the complex are faster than ^{1}H NMR time scale. Besides, the main driving force of the complexation is the hydrophobic interaction between the inner surface of Hy-α-CD ring and the hydrophobic site on CH_2CH_2O unit. This hydrophobic interaction causes deshielding effect on the methylene proton of the CH_2CH_2O unit and leads to signal of the methylene proton shifting downfield.

From curves in Figure 4a, it can be inferred that the methylene proton of THPEG for all samples shifts first upfield and then downfield and finally reaches equilibrium. This suggests that there is an assembly process between Hy-α-CD and THPEG. And it is time-consuming, which may be caused by the rearrangement process of threaded Hy-α-CDs on THPEG's chains. Hy-α-CDs thread onto THPEG's chains in despite of their positions and conformations as soon as THPEG is added. This process is fast and leads to large downfield shift at the beginning. Some Hy-α-CDs have improper state which is not energy minimum. Therefore, they dethread from THPEG's chains, adjust their conformations and positions, and then rethread. This process is relatively slow and time-consuming. It

DOI: 10.1021/acs.macromol.5b02359
Macromolecules XXXX, XXX, XXX−XXX

Scheme 2. Process of Complexation between THPEG and Hy-α-CD in Aqueous Solution and the Equilibrium State of the Poly-*Pseudo*-Rotaxane

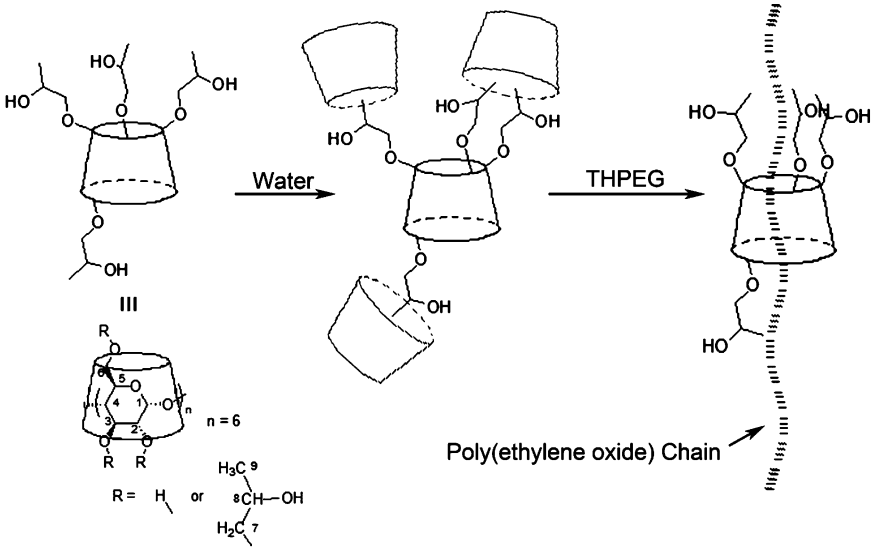

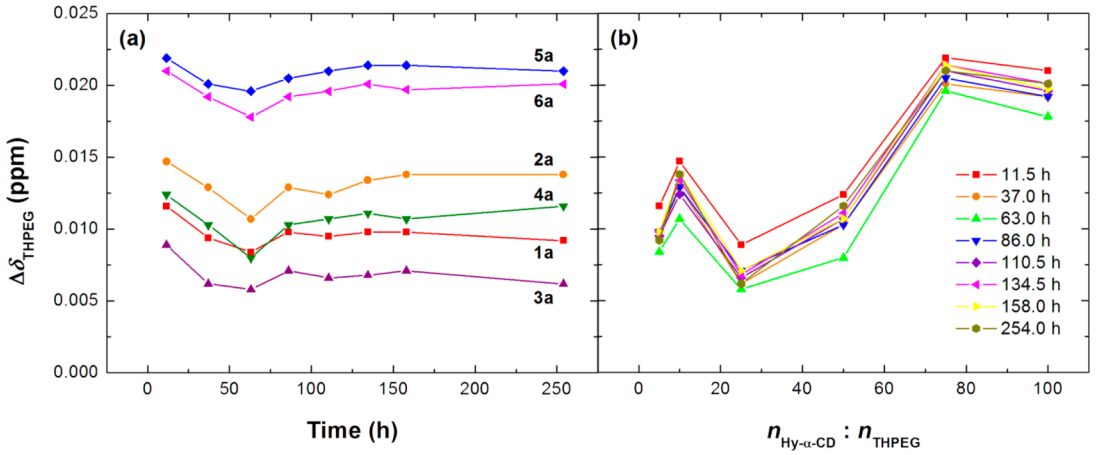

Figure 4. Chemical shift variations of THPEG's monomeric unit methylene protons ($\Delta\delta_{THPEG}$) as functions of (a) incubation time of samples **1a**–**6a** and (b) molar ratio of Hy-α-CD to THPEG ($n_{Hy\text{-}\alpha\text{-}CD}$:$n_{THPEG}$) with different incubation times.

is also found that different samples spend different time to reach the equilibrium. With increasing the value of $n_{Hy\text{-}\alpha\text{-}CD}$:$n_{THPEG}$, the time spent turns longer. This phenomenon can be easily understood that more Hy-α-CDs need more time to adjust their positions and conformations.

With the increase of the feed ratio of Hy-α-CD to THPEG ($n_{Hy\text{-}\alpha\text{-}CD}$:$n_{THPEG}$) from samples **1a** to **6a**, the value of $N_{Hy\text{-}\alpha\text{-}CD}$ increases monotonically in Table 2. However, the trend of the value of $\Delta\delta_{THPEG}$ from **1a** to **6a** is not consistent with that of $N_{Hy\text{-}\alpha\text{-}CD}$. Curves in Figure 4b show a strange pattern. In spite of differences on time, all the curves show an M-shaped trend.

When THPEG is added to Hy-α-CD's aqueous solution, they form poly-*pseudo*-rotaxane. Hy-α-CD can thread on and off of THPEG's chain dynamically, and this exchange is fast on a ^{1}H NMR time scale. When the value of $n_{Hy\text{-}\alpha\text{-}CD}$:$n_{THPEG}$ is small, all the fed Hy-α-CDs can thread on THPEG's chains. With the increase of $n_{Hy\text{-}\alpha\text{-}CD}$:$n_{THPEG}$, the threading ratio (SR) of Hy-α-CD decreases. When the value of $n_{Hy\text{-}\alpha\text{-}CD}$:$n_{THPEG}$ is small, the average number of Hy-α-CD corresponding to every arm of THPEG is small. For $n_{Hy\text{-}\alpha\text{-}CD}$:$n_{THPEG}$ is 5, the average number is 1.25. For $n_{Hy\text{-}\alpha\text{-}CD}$:$n_{THPEG}$ is 10, and the average number is 2.5. In these circumstances, Hy-α-CDs thread on and off the chains of THPEG freely and quickly with very few hampers. The exchange rate of THPEG between free and associated forms is high. Thus, the signal of methylene proton of THPEG locates relatively downfield. The methylene proton of THPEG of sample **2a** locates more downfield than that of **1a**. This is caused by the more Hy-α-CDs held by the poly-*pseudo*-rotaxane of **2a** than that of **1a** at the equilibrium. With $n_{Hy\text{-}\alpha\text{-}CD}$:$n_{THPEG}$ increasing to 25, the average number of Hy-α-CD threaded on every arm of THPEG increases to 5.5 thereupon. More Hy-α-CDs bring the threading/dethreading process some difficulties because of crowdedness, which slows the exchange of the poly-*pseudo*-rotaxane, and this is the main factor comparing with the increase of threaded Hy-α-CDs to determine the trend of the curve of $\Delta\delta_{THPEG} - n_{Hy\text{-}\alpha\text{-}CD}$:$n_{THPEG}$. So the methylene proton of THPEG shifts upfield. When $n_{Hy\text{-}\alpha\text{-}CD}$:$n_{THPEG}$ increases further, free THPEG disappears. THPEG's chains are covered by some Hy-α-CDs all along, which shortens the length of effective chains. Hy-α-CDs outside the chains can thread on and off, and this exchange turns fast again. Therefore, the methylene proton shifts downfield again. When $n_{Hy\text{-}\alpha\text{-}CD}$:$n_{THPEG}$ continuously increases from **5a** to **6a**, the main factor determine of trend of $\Delta\delta_{THPEG}$ turns to the reduced

DOI: 10.1021/acs.macromol.5b02359
Macromolecules XXXX, XXX, XXX−XXX

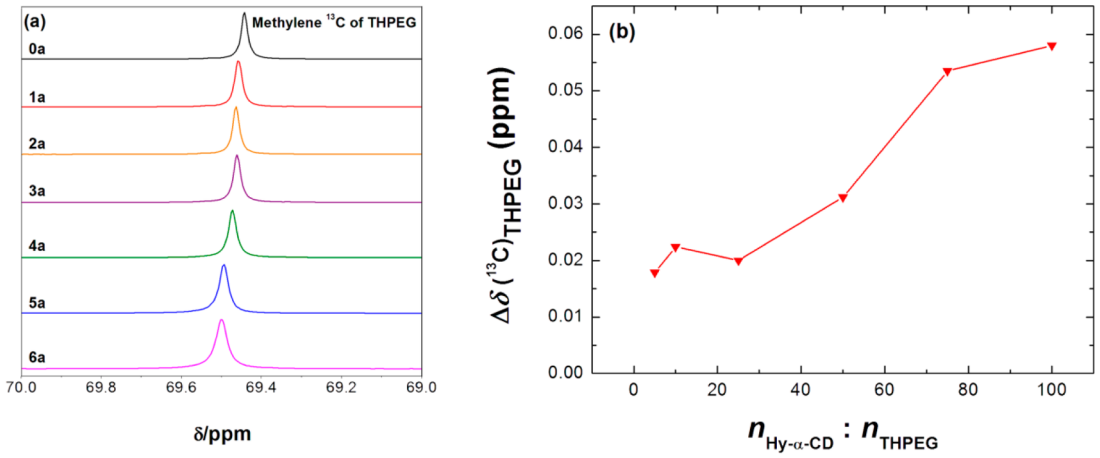

Figure 5. (a) Partial ^{13}C NMR spectra of samples **0a** to **6a** at dynamic equilibrium. (b) Chemical shift variations of ^{13}C of THPEG monomeric unit methylene $[\Delta\delta(^{13}C)_{THPEG}]$ as a functions of $n_{Hy\text{-}\alpha\text{-}CD}$:$n_{THPEG}$ at the equilibrium.

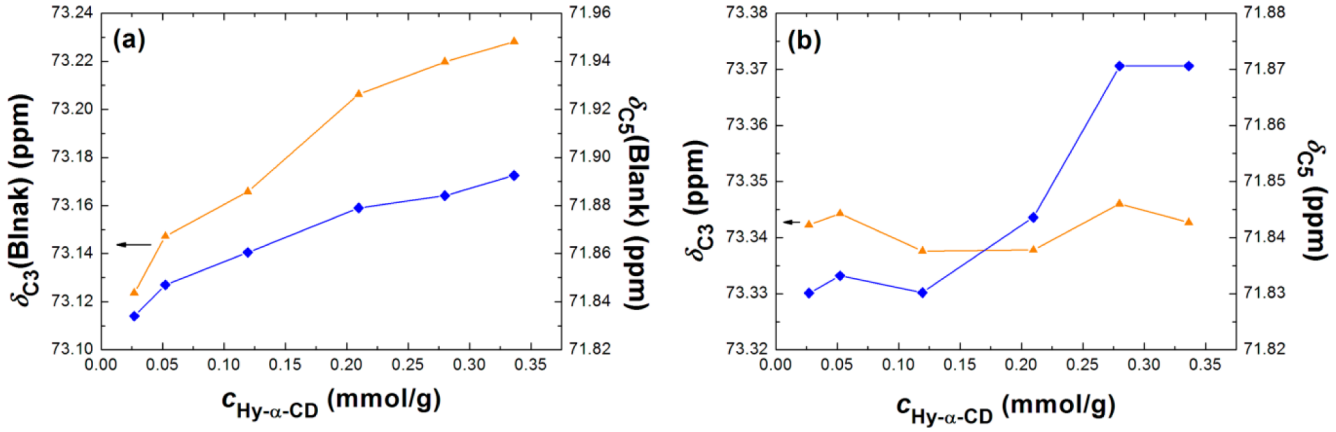

Figure 6. (a) Chemical shifts of carbons C3 $[\delta_{C3}(Blank)]$ and C5 $[\delta_{C5}(Blank)]$ of Hy-α-CD without THPEG as a function of mass concentration of Hy-α-CD ($c_{Hy\text{-}\alpha\text{-}CD}$). (b) Chemical shifts of carbons C3 (δ_{C3}) and C5 (δ_{C5}) of Hy-α-CD with THPEG as a function of $c_{Hy\text{-}\alpha\text{-}CD}$ at dynamic equilibrium.

exchange rate of the poly-*pseudo*-rotaxane again, so the value of $\Delta\delta_{THPEG}$ decreases again.

In short, though the trend of the value of $\Delta\delta_{THPEG}$ is inconsistent with that of $N_{Hy\text{-}\alpha\text{-}CD}$ with the increase of the feed ratio of Hy-α-CD to THPEG, this does not mean there is a mistake of calculated value of $N_{Hy\text{-}\alpha\text{-}CD}$. There are two factors determining the trend of $\Delta\delta_{THPEG}$, the amount of threaded Hy-α-CD, and the exchange rate of the poly-*pseudo*-rotaxane. These two factors have opposite effects on the trend of the curve of $\Delta\delta_{THPEG} - n_{Hy\text{-}\alpha\text{-}CD}$:$n_{THPEG}$. The M-shaped curve pattern of $\Delta\delta_{THPEG} - n_{Hy\text{-}\alpha\text{-}CD}$:$n_{THPEG}$ is the result of synergistic effect of the two factors.

Structure of Hy-α-CD/THPEG-Based Poly-Pseudo-Rotaxane at Dynamic Equilibrium. In ^{1}H NMR spectra of samples **0a** to **6a** at the dynamic equilibrium (Figure S1g,h), peaks of the methylene proton of THPEG broaden with the increase of $n_{Hy\text{-}\alpha\text{-}CD}$:$n_{THPEG}$, which indicates the chains of THPEG are covered by Hy-α-CD and the amount of Hy-α-CD threaded increases with the rise of $n_{Hy\text{-}\alpha\text{-}CD}$:$n_{THPEG}$. The broadness is related to the threading dynamics of PEO chain into the cavity of Hy-α-CD. When THPEG is threaded by Hy-α-CDs, the movements of all the molecules are restricted, and the flexibility of the PEO chains of THPEG reduces. In ^{13}C NMR spectra of **0a** to **6a** at the equilibrium (Figure 5a), the monomeric methylene carbon of THPEG exhibits signal around 69.4 ppm, and the peaks also broaden with the increase of $n_{Hy\text{-}\alpha\text{-}CD}$:$n_{THPEG}$. And the dependence of $\Delta\delta(^{13}C)_{THPEG}$ on $n_{Hy\text{-}\alpha\text{-}CD}$:$n_{THPEG}$ in Figure 5b is similar to curves in Figure 4b.

The Hy-α-CD used in this work has a substituted degree of 3.6, that is, 3.6 2-hydroxypropyl groups substitute randomly on C6, C3, or C2 positions on α-CD (Scheme 2). Unlike α-CD, hydrogen bonding within and between Hy-α-CDs is weakened due to the substitution. Therefore, in aqueous solution, Hy-α-CD has unique molecular conformations and behaviors with or without THPEG.

In ^{13}C NMR spectra, CD backbone carbons C3 and C5 of Hy-α-CD exhibit signals at around 73.2 and 71.8 ppm (Figure S4a,c), and methyl carbon C9 of the 2-hydroxypropyl group of Hy-α-CD exhibits a complex pattern at around 18.1 ppm (Figure S4b,d). Before the study of the poly-*pseudo*-rotaxane, behaviors of Hy-α-CDs in aqueous solution should be revealed because they can form intermolecular inclusion complexes with each other.

Figure 6a shows chemical shifts of carbons C3 $[\delta_{C3}(Blank)]$ and C5 $[\delta_{C5}(Blank)]$ of Hy-α-CD as a function of Hy-α-CD mass concentration ($c_{Hy\text{-}\alpha\text{-}CD}$) of blank references **1a(Blank)** to **6a(Blank)**. With the increase of $c_{Hy\text{-}\alpha\text{-}CD}$, δ_{C3}(Blank) and δ_{C5}(Blank) shift downfield gradually, and the curve of δ_{C3}(Blank) $- c_{Hy\text{-}\alpha\text{-}CD}$ is steeper than the curve of δ_{C5}(Blank) $- c_{Hy\text{-}\alpha\text{-}CD}$. These results indicate that Hy-α-CDs form inclusion

DOI: 10.1021/acs.macromol.5b02359
Macromolecules XXXX, XXX, XXX−XXX

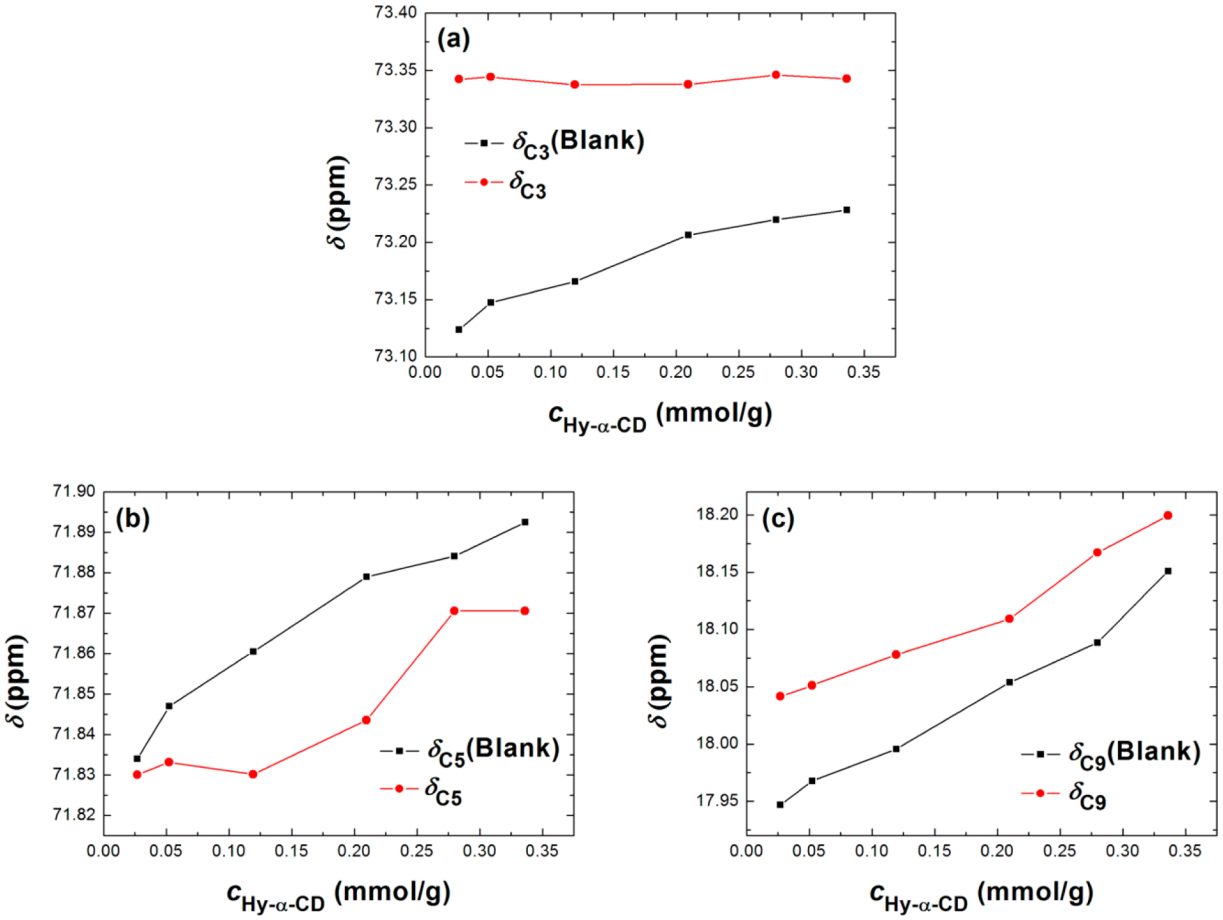

Figure 7. Chemical shifts of carbons C3 (a), C5 (b), and C9 (c) of Hy-α-CD with and without THPEG as functions of mass concentration of Hy-α-CD ($c_{Hy\text{-}\alpha\text{-}CD}$).

complexes. In addition, δ_{C3}(Blank) and δ_{C5}(Blank) show concentration dependency, so the chemical shift variations cannot be attributed to the formation of intramolecular complex.[41] The methyl part on the 2-hydroxypropyl group of one Hy-α-CD can insert into the cavity of another Hy-α-CD shallowly from both wide and narrow rims driven by hydrophobic interaction. Owing to sizes' difference, the wide rim of Hy-α-CD is able to accommodate more than one methyl group while the narrow rim does only one. Carbon C3 which is closer to the wide rim interacts with more methyl groups than C5 does, causing larger gradient of the curve. δ_{C9}(Blank) shows similar concentration dependency which also demonstrates the existence of the intermolecular inclusion complexes (Figure 7c, black line).

When THPEG is added, for samples **1a** to **6a**, in Figure 7, δ_{C3} and δ_{C9} shift downfield, whereas δ_{C5} shifts upfield for all $c_{Hy\text{-}\alpha\text{-}CD}$. In aqueous solution without THPEG, Hy-α-CDs form inclusion complexes. When THPEG is added, the inclusion complexes dissociate, and the free Hy-α-CDs complex with THPEG to form poly-*pseudo*-rotaxane. In this process, both methines of C3 and C5 experience the transition that the group they interact with changes from methyl ($-CH_3$) of 2-hydroxypropyl to ethylene oxide unit (CH_2CH_2O) of THPEG. In the cavity of Hy-α-CD, methine of C3 is closer to the wide rim, whereas methine of C5 is closer to the narrow rim. For the methine of C5, the interaction between it and the methyl group is stronger than that between it and the ethylene oxide group due to the better size matchment between the narrow rim of Hy-α-CD and methyl. So on addition of THPEG, change of guest group from methyl of 2-hydroxypropyl to ethylene oxide unit of THPEG leads to signal of carbon C5 shifting upfield. For the methine of C3, the methyl of 2-hydroxypropyl group complex with it loosely in the inclusion complex formed by Hy-α-CDs because the size of wide rim of Hy-α-CD is slightly larger for the methyl group. On addition of THPEG, Hy-α-CD threads on the PEO chain and complexes with it tightly due to the formation of the pseudorotaxane mechanical bond. So the interaction between the methine of C3 and ethylene oxide of THPEG is stronger compared with that of methine of C3 and the methyl group in the inclusion complex. This results in signal of C3 shifting downfield after the addition of THPEG. Curves of $\delta_{C3} - c_{Hy\text{-}\alpha\text{-}CD}$ and $\delta_{C5} - c_{Hy\text{-}\alpha\text{-}CD}$ show M-shaped trend, which is similar to curves of $\Delta\delta_{THPEG} - n_{Hy\text{-}\alpha\text{-}CD}{:}n_{THPEG}$. Moreover, the slope of the $\delta_{C5}{-}c_{Hy\text{-}\alpha\text{-}CD}$ curve surpasses that of the $\delta_{C3}{-}c_{Hy\text{-}\alpha\text{-}CD}$ curve (Figure 6b). These results indicate that Hy-α-CD threads on THPEG's chains.

From the results of ATR-FTIR and XPS above, it reaches a conclusion that Hy-α-CD is confined in the network of the αSSS hydrogel and the confined Hy-α-CD cannot be washed away by water. This is most likely caused by the formation of poly-*pseudo*-rotaxane between Hy-α-CD and tetra-PEG macromonomers in pregel solution, and the threaded Hy-α-CD is confined in the network of the hydrogel after gelation of the poly-*pseudo*-rotaxane. And the results of 2D NOESY, ^{1}H and ^{13}C NMR confirmed this speculation. Based on the ATR, XPS,

DOI: 10.1021/acs.macromol.5b02359
Macromolecules XXXX, XXX, XXX−XXX

and NMR results and the discussion above, the clarified mechanism of the complexation between THPEG and Hy-α-CD in aqueous solution is depicted in Scheme 2. Before THPEG is added, Hy-α-CDs form intermolecular inclusion complexes. The methyl part on 2-hydroxypropyl group of one Hy-α-CD inserts shallowly in the cavity of another Hy-α-CD from wide or narrow rims. The wide rim can accommodate more than one methyl group, whereas the narrow rim can hold only one. Hy-α-CDs thread onto THPEG's chains as soon as THPEG is added irrespective of their positions and conformations. After that, some Hy-α-CDs dethread from THPEG's chains, regulate their conformations and positions, and rethread. This process is time-consuming. The time needed to reach dynamic equilibrium increases with the increase of the feed ratio ($n_{\text{Hy-}\alpha\text{-CD}}$:$n_{\text{THPEG}}$). At the equilibrium, THPEG is covered by Hy-α-CDs 2-hydroxypropyl groups of which are parallel with THPEG's chain and have interaction with it. The amount of Hy-α-CD threaded on THPEG at the equilibrium increases with the increase of $n_{\text{Hy-}\alpha\text{-CD}}$:$n_{\text{THPEG}}$, though the threading ratio of Hy-α-CD decreases with the increase of the feed ratio. When the amount of fed Hy-α-CD is small, all of them can thread onto THPEG's chains. This is the result of strong interaction between Hy-α-CD and poly(ethylene oxide) chain. When more Hy-α-CDs are added, not all of them can thread onto THPEG's chains, which is the consequences of crowdedness effect and dynamic equilibrium between threading and dethreading Hy-α-CD. Some Hy-α-CDs unthread all along.

On the basis of extensive investigation of the mechanism of complexation between Hy-α-CD and tetra-PEG macromonomer, we are able to understand the relationship between the structure of Hy-α-CD/tetra-PEG macromonomer based poly-*pseudo*-rotaxane and the composition of αSSS hydrogel. And the amount of Hy-α-CD introduced into the αSSS hydrogel can be controlled easily by tuning the feed ratio.

Internal Morphology of the αSSS Hydrogel. Figure 8 shows typical SEM images of sectioned surfaces of pristine

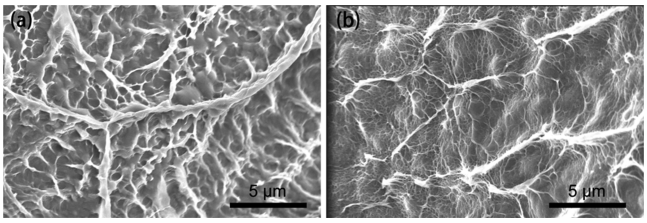

Figure 8. SEM images of the sectioned surfaces of freeze-dried hydrogels (a) **0ag** and (b) **5ag**.

tetra-PEG gel **0ag** and αSSS hydrogel **5ag**. **0ag** has homogeneous network with thick and loose texture, whereas, **5ag**'s network appears slim and fine texture. Poly(ethylene oxide) has strong tendency to get together and crystallize. In freeze-dried tetra-PEG hydrogel's network, chains of poly(ethylene oxide) gather to form thick texture. When Hy-α-CDs are introduced, they cover poly(ethylene oxide) chain of the network, hinder the approach among the chains, and weaken the crystallization. Moreover, the rigidity of the chain rises due to the coverage of Hy-α-CDs.

Mechanical Properties of the αSSS Hydrogel. Compression test was performed to investigate mechanical properties of the αSSS hydrogel.

In Figure 9, the points at N_{Initial} = 0 represent pristine tetra-PEG gel **0ag**; the points at N_{initial} = 5, 10, 25, 50, 75, and 100

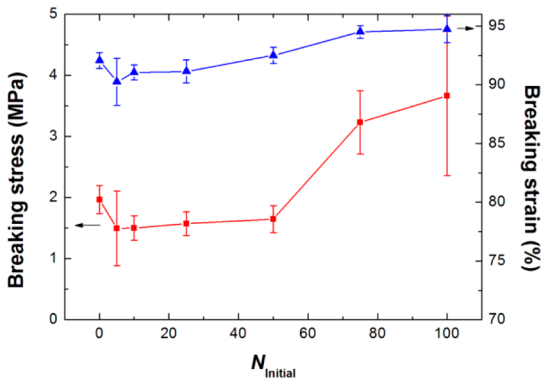

Figure 9. Molar ratio of Hy-α-CD to THPEG (N_{Initial}) dependence of breaking stress (red square) and breaking strain (blue triangle).

represent αSSS hydrogels **1ag**, **2ag**, **3ag**, **4ag**, **5ag**, and **6ag**. The breaking stresses of the αSSS hydrogels are in the same order of magnitude as that of the tetra-PEG gel, which also partly indicates the homogeneous network of tetra-PEG gel is inherited by the αSSS hydrogel, for the ideal network structure is the origin of the high mechanical strength of the tetra-PEG gel. We can find that the breaking stresses of the αSSS hydrogels **1ag** to **4ag** are slightly lower than that of **0ag**. But when more Hy-α-CDs are added, the strength of the αSSS hydrogel surpasses that of tetra-PEG gel and even up to 3.67 MPa. The existence of large amount of Hy-α-CD increases the stiffness of the network chains in the hydrogel, which leads to the high strength. Both the pristine tetra-PEG gel and the αSSS hydrogel have high breaking strain over 90%, which indicates these hydrogels of excellent flexibilities.

Sakai and co-workers reported in 2010 a tetra-PEG gel with compression breaking strength of 27 MPa.[43] Compression properties of tetra-PEG hydrogel **0ag** and αSSS hydrogels **1ag** to **6ag** in present study are not as good as the tetra-PEG gel of Sakai's. This may be the results of different cross-linking reactions and preparing conditions of the hydrogels and different samples' states in compression test. The tetra-PEG gel reported by Sakai et al. was prepared through termini cross-coupling of amine and NHS-glutarate groups, whereas the tetra-PEG and αSSS hydrogel here were prepared through "CuAAC" click gelation reaction. The cross-linking media of Sakai's tetra-PEG gel is mixture of phosphate and phosphate−citric acid buffers, whereas the cross-linking media of tetra-PEG and αSSS hydrogels here is DI water. The last but perhaps most important factor is that the hydrogel specimen being executed with compression test was used in as-prepared state in the work reported by Sakai and co-workers, whereas here the tetra-PEG and αSSS hydrogels were fully swollen before the compression test. So the compression strengths of hydrogels reported here are different from that of tetra-PEG gel reported by Sakai et al.

Introduction of a Function into αSSS Hydrogel. In the last part, a function was introduced into the αSSS hydrogel to preliminarily study the validity of the potential functionalization sites of Hy-α-CD. Anthracene was chosen as an example of the function. It was chemically linked to Hy-α-CD, and the resultant An-Hy-α-CD (Scheme 3) was complexed with tetra-PEG macromonomers TAPEG and TPPEG. The resulted poly-*pseudo*-rotaxane was then cross-linked through "CuAAC" click chemistry to obtain the An-αSSS hydrogel. The hydrogel was treated with EDTA-2Na aqueous solution to remove the catalyst and then repeated washed with water and DMF until

DOI: 10.1021/acs.macromol.5b02359
Macromolecules XXXX, XXX, XXX−XXX

Scheme 3. Molecular Structure of An-Hy-α-CD

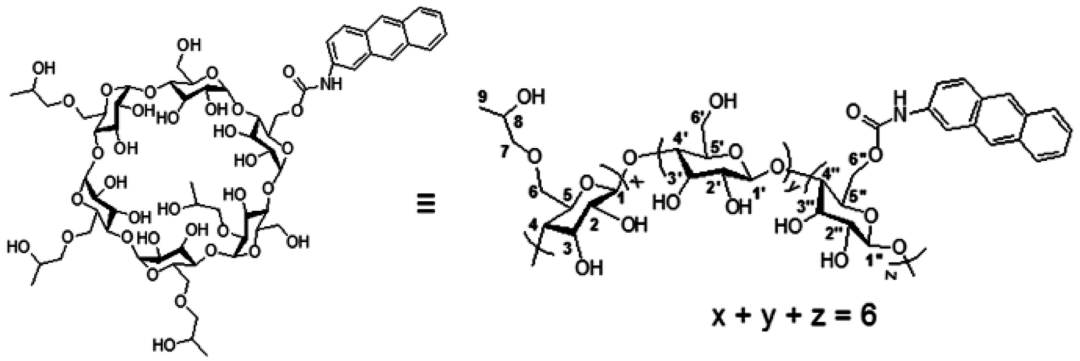

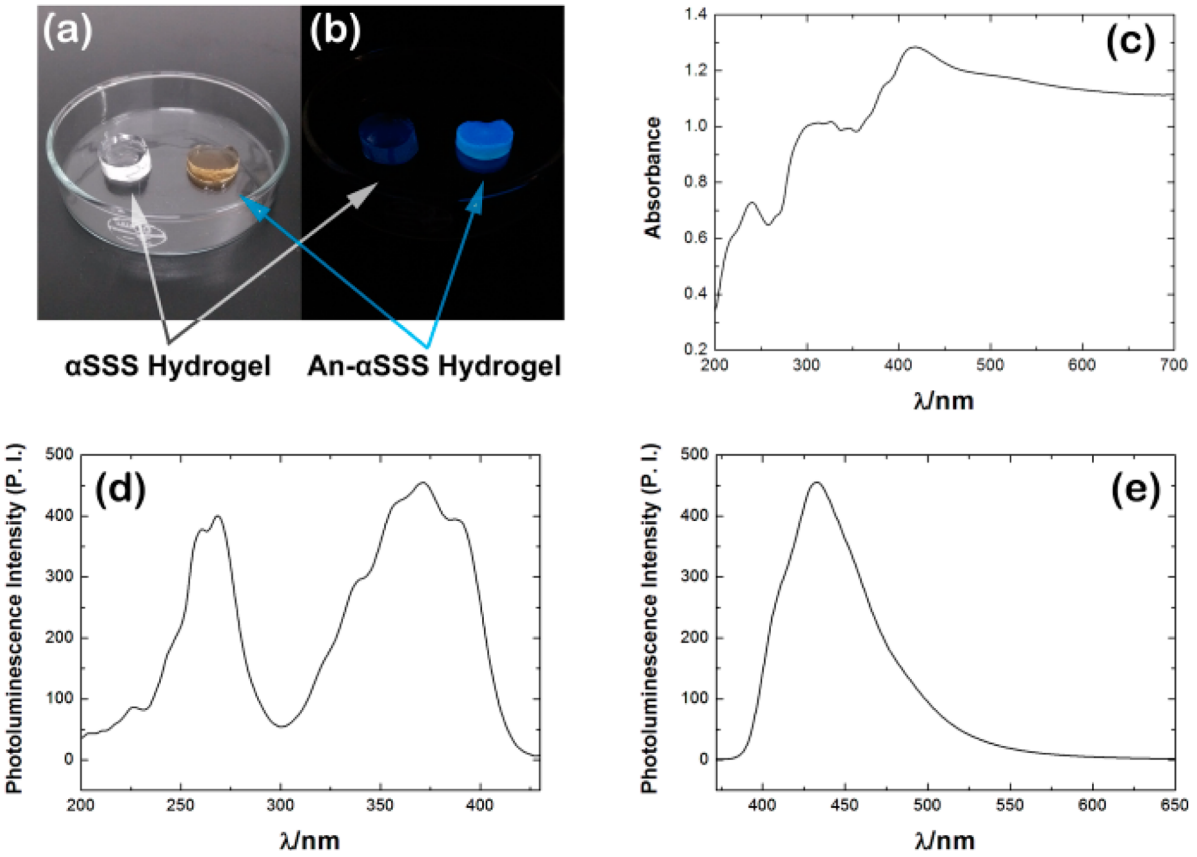

Figure 10. Photographs of αSSS hydrogel and An-αSSS hydrogel under (a) daylight and (b) 365 nm UV illumination. (c) UV−vis DRS spectrum of An-αSSS hydrogel. (d) Fluorescent excitation spectrum of An-αSSS hydrogel. (e) Fluorescent emission spectrum of An-αSSS hydrogel.

no unthreaded An-Hy-α-CD residue was remained. The hydrogel was fully swollen in DI water before characterizations.

Figure 10a,b shows photographs of αSSS hydrogel and An-αSSS hydrogel under daylight and 365 nm UV illumination. Under daylight An-αSSS hydrogel presents brown color compared with the colorless αSSS hydrogel. Under the UV illumination An-αSSS hydrogel emits blue fluorescent light. In the UV−vis DRS spectrum of An-αSSS hydrogel (Figure 10c), the low-energy band of the ^1B_b transition of anthracene unit appears around 240 nm, and the ^1L_a band appears between 260 and 360 nm.[44] Figure 10d shows excitation spectrum of An-αSSS hydrogel. From the figure, a excitation wavelength of 360 nm was chosen to further record the emission spectrum of An-αSSS hydrogel in Figure 10e which is in agreement with the emission curve of anthracene unit.[45] The results above all indicate that the functional unit of anthracene was successfully introduced into the αSSS hydrogel through functionalization site of Hy-α-CD and the obtained An-αSSS hydrogel possesses fluorescent character. Extensive investigation of preparation, characterization, and functional feature of the An-αSSS hydrogel system is in progress in our laboratory.

Functionalizing the αSSS hydrogel with anthracene unit is an attempt to utilize the potential functionalization site of Hy-α-CD in the hydrogel. Further study of functionalization of the αSSS hydrogel with other diverse functions is under way.

CONCLUSION

A novel tetra-PEG/Hy-α-CD hydrogel with a homogeneous network and tunable potential functionalization sites has been successfully prepared. Tetra-PEG gel as the skeleton endows

DOI: 10.1021/acs.macromol.5b02359
Macromolecules XXXX, XXX, XXX−XXX

the hydrogel with an ideal network structure and good mechanical properties. Evenly distributed Hy-α-CDs as the functionalization sites thread on poly(ethylene oxide) chain and can shuttle between two cross-linking points. Formation of poly-*pseudo*-rotaxane with Hy-α-CD and tetra-PEG macromonomers is the critical stage for the preparation of the hydrogel, for the amount of Hy-α-CD introduced is in relation with the structure of the poly-*pseudo*-rotaxane. The amount of Hy-α-CD introduced into the hydrogel can be controlled easily by tuning the feed ratio. The got αSSS hydrogels composed by biocompatible tetra-PEG macromonomers and Hy-α-CD have higher mechanical strengths. So it is believed that the hydrogel has great potential in biomedical applications.

Besides, anthracene as an example of function was successfully introduced into the αSSS hydrogel through Hy-α-CD, which preliminarily verifies the feasibility of using Hy-α-CD as the functionalization site. The constructed An-αSSS hydrogel has character of fluorescence.

Thus, we think that a feasible method has been found to prepare a new hydrogel having both better mechanical properties and diverse functionalities. The αSSS hydrogel could be a platform to be modified easily and turned to functional materials due to the tunable functionalization sites of Hy-α-CDs. And also the resultant slidable functions may bring the hydrogel new properties. Further work is in progress.

■ ASSOCIATED CONTENT

Supporting Information

The Supporting Information is available free of charge on the ACS Publications website at DOI: 10.1021/acs.macromol.5b02359.

Synthesis scheme for tetra-azido-terminated PEG (TAPEG) and tetra-propargyl-terminated PEG (TPPEG), ^{1}H NMR spectra of samples **0a** to **6a** with incubation time involved in Figure 1, ^{1}H NMR spectra of reference samples **1a(Blank)** to **6a(Blank)**, ^{13}C NMR spectra of samples **0a** to **6a** at equilibrium, and ^{13}C NMR spectra of reference samples **1a(Blank)** to **6a(Blank)** (PDF)

■ AUTHOR INFORMATION

Corresponding Author

*Ph +86-21-54745817; e-mail xlwang@sjtu.edu.cn (X.W.).

Notes

The authors declare no competing financial interest.

■ ACKNOWLEDGMENTS

This work is financially supported by National Natural Science Foundation of China (21274085) and Shanghai Leading Academic Discipline Project (no. B202). The author is grateful for support from Evonik Degussa (China) Co., Ltd.

■ REFERENCES

(1) Kamata, H.; Akagi, Y.; Kayasuga-Kariya, Y.; Chung, U.; Sakai, T. *Science* **2014**, *343*, 873−875.
(2) Lin, C. C.; Metters, A. T. *Adv. Drug Delivery Rev.* **2006**, *58*, 1379−1408.
(3) Kogan, G.; Soltes, L.; Stern, R.; Gemeiner, P. *Biotechnol. Lett.* **2007**, *29*, 17−25.
(4) Dong, L.; Agarwal, A. K.; Beebe, D. J.; Jiang, H. R. *Nature* **2006**, *442*, 551−554.
(5) Lee, E.; Kim, B. *Korean J. Chem. Eng.* **2011**, *28*, 1347−1350.
(6) Li, X. Y.; Lin, Y. *Environ. Chem.* **2010**, *29*, 305−309.
(7) Shibayama, M. *Soft Matter* **2012**, *8*, 8030−8038.
(8) Haraguchi, K.; Takehisa, T. *Adv. Mater.* **2002**, *14*, 1120−1124.
(9) Huang, T.; Xu, H. G.; Jiao, K. X.; Zhu, L. P.; Brown, H. R.; Wang, H. L. *Adv. Mater.* **2007**, *19*, 1622−1626.
(10) Gong, J. P.; Katsuyama, Y.; Kurokawa, T.; Osada, Y. *Adv. Mater.* **2003**, *15*, 1155−1158.
(11) Okumura, Y.; Ito, K. *Adv. Mater.* **2001**, *13*, 485−487.
(12) Bin Imran, A.; Esaki, K.; Gotoh, H.; Seki, T.; Ito, K.; Sakai, Y.; Takeoka, Y. *Nat. Commun.* **2014**, *5*, 5124.
(13) Mayumi, K.; Tezuka, M.; Bando, A.; Ito, K. *Soft Matter* **2012**, *8*, 8179−8183.
(14) Sakai, T.; Matsunaga, T.; Yamamoto, Y.; Ito, C.; Yoshida, R.; Suzuki, S.; Sasaki, N.; Shibayama, M.; Chung, U. I. *Macromolecules* **2008**, *41*, 5379−5384.
(15) Matsunaga, T.; Sakai, T.; Akagi, Y.; Chung, U. I.; Shibayama, M. *Macromolecules* **2009**, *42*, 1344−1351.
(16) Matsunaga, T.; Sakai, T.; Akagi, Y.; Chung, U. I.; Shibayama, M. *Macromolecules* **2009**, *42*, 6245−6252.
(17) Nishi, K.; Fujii, K.; Katsumoto, Y.; Sakai, T.; Shibayama, M. *Macromolecules* **2014**, *47*, 3274−3281.
(18) Akagi, Y.; Gong, J. P.; Chung, U. I.; Sakai, T. *Macromolecules* **2013**, *46*, 1035−1040.
(19) Shibayama, M. *J. Phys. Soc. Jpn.* **2009**, *78*, 041008−1−7.
(20) Nomoto, Y.; Matsunaga, T.; Sakai, T.; Tosaka, M.; Shibayama, M. *Polymer* **2011**, *52*, 4123−4128.
(21) Jia, H.; Li, Z.; Wang, X.; Zheng, Z. *J. Mater. Chem. A* **2015**, *3*, 1158−1163.
(22) Wenz, G.; Han, B. H.; Muller, A. *Chem. Rev.* **2006**, *106*, 782−817.
(23) Wenz, G. *Angew. Chem., Int. Ed. Engl.* **1994**, *33*, 803−822.
(24) Easton, C. J.; Lincoln, S. F. *Modified Cyclodextrins, Scaffolds and Templates for Supramolecular Chemistry*; Imperial College Press: London, 1999; p 72.
(25) Harada, A.; Hashidzume, A.; Yamaguchi, H.; Takashima, Y. *Chem. Rev.* **2009**, *109*, 5974−6023.
(26) Harada, A.; Kamachi, M. *Macromolecules* **1990**, *23*, 2821−2823.
(27) Murata, N.; Konda, A.; Urayama, K.; Takigawa, T.; Kidowaki, M.; Ito, K. *Macromolecules* **2009**, *42*, 8485−8491.
(28) Noda, Y.; Hayashi, Y.; Ito, K. *J. Appl. Polym. Sci.* **2014**, *131*, 40509.
(29) Maestrelli, F.; Garcia-Fuentes, M.; Mura, P.; Alonso, M. J. *Eur. J. Pharm. Biopharm.* **2006**, *63*, 79−86.
(30) Uliniuc, A.; Popa, M.; Hamaide, T.; Dobromir, M. *Cell Chem. Technol.* **2012**, *46*, 1−11.
(31) Kolb, H. C.; Finn, M. G.; Sharpless, K. B. *Angew. Chem., Int. Ed.* **2001**, *40*, 2004−2021.
(32) de Miranda, M. G.; de Oliveira, M. F. G.; Lopes, R. S. C.; da Silva, A. J. R.; Albert, A. L. M.; Lopes, C. C. *Tetrahedron Lett.* **2013**, *54*, 2587−2590.
(33) Polizzotti, B. D.; Fairbanks, B. D.; Anseth, K. S. *Biomacromolecules* **2008**, *9*, 1084−1087.
(34) Xu, L. Q.; Yao, F.; Fu, G. D.; Kang, E. T. *Biomacromolecules* **2010**, *11*, 1810−1817.
(35) Alston, D. R.; Lilley, T. H.; Stoddart, J. F. *J. Chem. Soc., Chem. Commun.* **1985**, 1600−1602.
(36) Funasaki, N.; Nomura, M.; Yamaguchi, H.; Ishikawa, S.; Neya, S. *Bull. Chem. Soc. Jpn.* **2000**, *73*, 2727−2728.
(37) Schneider, H. J.; Hacket, F.; Rudiger, V.; Ikeda, H. *Chem. Rev.* **1998**, *98*, 1755−1785.
(38) Ennist, J. H.; Gobrogge, E. A.; Schlick, K. H.; Walker, R. A.; Cloninger, M. J. *ACS Appl. Mater. Interfaces* **2014**, *6*, 18087−18097.
(39) Sun, T. L.; Kurokawa, T.; Kuroda, S.; Bin Ihsan, A.; Akasaki, T.; Sato, K.; Haque, M. A.; Nakajima, T.; Gong, J. P. *Nat. Mater.* **2013**, *12*, 932−937.
(40) Harada, A.; Takashima, Y.; Yamaguchi, H. *Chem. Soc. Rev.* **2009**, *38*, 875−882.
(41) Inoue, Y.; Miyauchi, M.; Nakajima, H.; Takashima, Y.; Yamaguchi, H.; Harada, A. *Macromolecules* **2007**, *40*, 3256−3262.
(42) Duhamel, J. *Acc. Chem. Res.* **2006**, *39*, 953−960.

DOI: 10.1021/acs.macromol.5b02359
Macromolecules XXXX, XXX, XXX−XXX

(43) Sakai, T.; Akagi, Y.; Matsunaga, T.; Kurakazu, M.; Chung, U. I.; Shibayama, M. *Macromol. Rapid Commun.* **2010**, *31*, 1954−1959.
(44) Yang, C.; Mori, T.; Origane, Y.; Ko, Y. H.; Selvapalam, N.; Kim, K.; Inoue, Y. *J. Am. Chem. Soc.* **2008**, *130*, 8574−8575.
(45) Nakamura, A.; Inoue, Y. *J. Am. Chem. Soc.* **2003**, *125*, 966−972.

DOI: 10.1021/acs.macromol.5b02359
Macromolecules XXXX, XXX, XXX−XXX